

Research paper

Precise measurement of junction temperature by thermal analysis of light-emitting diode operated at high environmental temperature

Hyunjin Choi^a, Leilei Wang^a, Seok-Won Kang^b, Jiseok Lim^{a,*}, Jungwook Choi^{a,*}^a School of Mechanical Engineering, Yeungnam University, 280 Daehak-ro, Gyeongsan, Gyeongbuk 38541, Republic of Korea^b Department of Automotive Engineering, Yeungnam University, 280 Daehak-ro, Gyeongsan, Gyeongbuk 38541, Republic of Korea

ARTICLE INFO

Keywords:

Light-emitting diode
High-temperature environment
Junction temperature
Phosphor temperature
Thermal resistance
Thermal management

ABSTRACT

Light-emitting diodes (LEDs) have become a promising solid-state light source in numerous applications. During operation, they are often exposed to high environmental temperatures, resulting in performance and reliability degradation. It is thus important to monitor the temperature at the junction, which is a primary lighting and heat source, especially for an LED operated under a high-temperature environment. In this study, the temperatures at the junction, phosphor, and thermal pad of the LED operated at high temperatures (up to 107.2 °C) are measured and analyzed. The junction temperature is measured by a transient thermal tester at known environmental temperatures and input currents. Moreover, the temperatures at the phosphor and thermal pad are simultaneously measured by using an infrared (IR) thermometer and a thermocouple, respectively. A single highly linear temperature correlation ($R^2 = 0.997$) is found between the junction and phosphor temperatures regardless of the operating conditions. This could aid in precisely estimating the junction temperature by simply measuring the surface temperature of phosphor. On the other hand, the correlation between the junction and thermal pad temperature that is often treated as a single correlation exhibits dependence on the input current over the tested temperature range. The structural thermal analysis on the thermal resistance of the LED package supports the experimental results along with the numerical analysis. The obtained results in this study could provide a set of guidelines for the precise prediction of junction temperature and thermal management of LEDs, which are operated under high-temperature environments.

1. Introduction

Light-emitting diodes (LEDs) are widely used in many industrial fields, given its low power consumption, high performance, long lifetime, and wide color temperature [1]. Recently, the phosphor-converted LED has become a promising candidate as a white light source for automotive headlamps [2]. In such applications, a higher power output and an improved reliability against harsh operating environments (including shock, vibration, and high temperature and humidity) are required [3]. The increase in optical output inevitably results in the increase in junction temperature because a significant amount of input power is converted into heat at a p-n junction [4]. In particular, the junction temperature would further increase when the LED is operated in an elevated ambient temperature (e.g., headlamp application).

The p-n junction of an LED is the primary heat source, and the optical performance and reliability of the LED module are dependent on the junction temperature. An increased junction temperature causes the degradation of LED efficiency and lifetime as well as the shift in

emission wavelength [5–8]. The decrease in efficiency can be accelerated when the LED is continuously exposed to a high-temperature environment. Moreover, the heat can be accumulated at solder joints, resulting in failure by oxidation, crack generation, and solder delamination [9–12]. In the case of a phosphor-converted LED, the phosphor conversion efficiency also decreases with temperature increase [13,14], and phosphor self-heating could augment more heat to the LED package [15–17]. The precise measurement of the LED junction temperature would thus be a starting point for the selection and design other components, such as the heat sink [18–22], especially for LEDs operated in high-temperature environments. Apart from the junction temperature, the phosphor temperature must also be considered for the successful thermal management of the entire LED package [23,24].

A few techniques have been investigated to measure the temperature and characterize the thermal behavior of LED packages. Among the many approaches, thermocouples are widely used to measure the temperature of a specific location on the LED surface. Although the absorption of optical energy by thermocouples could lead to inaccuracy

* Corresponding authors.

E-mail addresses: jlim@yu.ac.kr (J. Lim), jwc@yu.ac.kr (J. Choi).

[25], its simplicity and low cost enable the evaluation of junction temperature when the input power and thermal resistance are known. In contrast to the thermocouple, which requires surface contact, a few non-contact techniques have also been used for the thermal characterization of LEDs. The junction temperature can be measured by optical spectroscopy based on the shift in Raman and luminescence signatures [26,27], whereas the infrared (IR) camera provides a visualization of the temperature profile on the LED surface [28–30]. Furthermore, the forward voltage method and transient thermal tester, which utilizes the temperature dependence of forward voltage, also provide the value of junction temperature as a function of input power [31–38]. Although non-contact methods require complex equipment and systems, these allow the measurement of junction temperature with high accuracy. Regardless of measurement procedures, however, most investigations on the LED junction temperature have been conducted at room temperature. Although a few studies have reported the temperature-dependent optical performance of LEDs [39–42], the precise measurement of the junction temperature in a high-temperature environment is also important, considering that high-temperature operations significantly limit the lifetime and degrades the optical output of LEDs [43–47].

In this work, the junction, phosphor, and surface (*i.e.*, copper thermal pad on a substrate) temperatures of the LED package exposed to high environmental temperatures and various input currents are measured and characterized. The junction temperature is measured by a commercial transient thermal tester (*e.g.*, T3Ster) [48], whereas the phosphor temperature is measured by an IR camera at identical driving currents and environmental temperatures. At the same time, the temperature on the thermal pad is measured using a thermocouple. This method can be potentially used for general and practical purposes in the LED-based product design and characterization. A series of experiments demonstrates a single correlation between the junction and phosphor temperatures with high linearity ($R^2 = 0.997$) in the temperature range 30–150 °C regardless of input currents. On the other hand, the temperature of the thermal pad shows input current-dependent linear correlations ($R^2 = 0.999$ for all tested input currents) with the junction temperature over the tested temperature range. This indicates that the input current must be considered to measure the junction temperature from the thermal pad temperature. These empirical correlations are supported by numerical analysis. In addition, the structural thermal analysis of the LED package confirms that the thermal resistance from the junction to the phosphor and thermal pad can be changed due to a change in thermal conductivity according to the operational conditions, which should also be considered for successful thermal characterization. The obtained results are anticipated to be useful for effective thermal management and securing the reliability of LED packages operated in a high-temperature environment.

2. Experiment

In order to measure and characterize the temperatures of junction, phosphor, and thermal pad of the LED package at an elevated temperature, a temperature controllable convection oven with an IR transparent window and electrical feedthrough is custom-built. The phosphor-converted white-light LED mounted on an aluminum substrate with a thermal clad as a dielectric is placed inside the oven. For efficient heat dissipation, an aluminum heatsink is attached at the bottom of the LED package. As described in Fig. 1(a), the temperatures at the junction, phosphor, and copper thermal pad at a high environmental temperature range of 24.8–107.2 °C are measured by T3Ster (Mentor Graphics), IR camera (FLIR A310), and K-type thermocouple equipped with a digital multimeter (Keithly 2000), respectively. It should be noted that the actual temperature exposure of the LED is simultaneously measured by another thermocouple placed near the LED package. Based on measured temperature values as a function of input currents and environmental temperatures, the junction–phosphor and

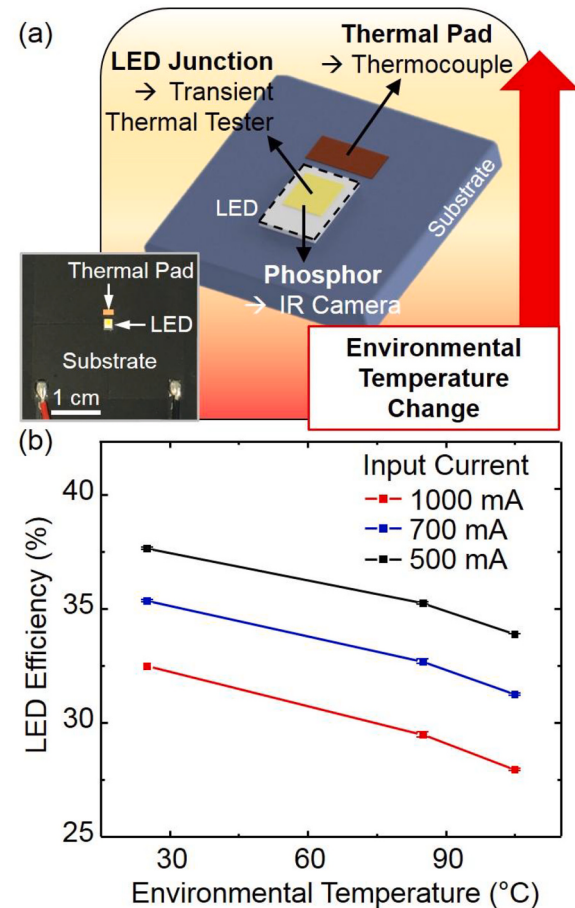


Fig. 1. Schematic of LED package and experimental methods for its thermal characterization at a high environmental temperature. (a) The temperatures of LED junction, phosphor, and thermal pad are measured and analyzed at various input currents and high environmental temperatures up to 107.2 °C. Different instruments (T3Ster, IR thermometer, and thermocouple) are employed to measure the LED temperature at each location. The inset shows the optical image of the LED. (b) LED efficiency measured at various input currents and environmental temperatures. As the current and temperature increase up to 1000 mA and 105 °C, respectively, the efficiency significantly decreases to 27.95%, indicating the significant effect of temperature on LED performance.

junction–thermal pad temperature correlations are found. These correlations allow the precise estimation of the junction temperature by simply measuring the temperatures of the phosphor or thermal pad at a given environmental temperature.

The effect of increased temperature on the LED is firstly verified by measuring its efficiency with respect to the input currents in the range 500–1000 mA. The efficiency is defined as the optical output power per electrical input power and measured by an integrating sphere with controllable temperature. As shown in Fig. 1(b), the increase in environmental temperature gradually degrades the efficiency at the identical input current. Additionally, the increase in input current also decreases the efficiency because more heat is generated at the junction, thereby eventually increasing the temperature of the LED package. This tendency, which is consistent with that in a previous report [6], highlights the importance of the effective thermal management of the LED package to maintain its performance. In this context, the temperatures at the junction, phosphor, and thermal pad of the LED exposed to high temperature are systematically characterized to precisely evaluate the thermal profile across the LED.

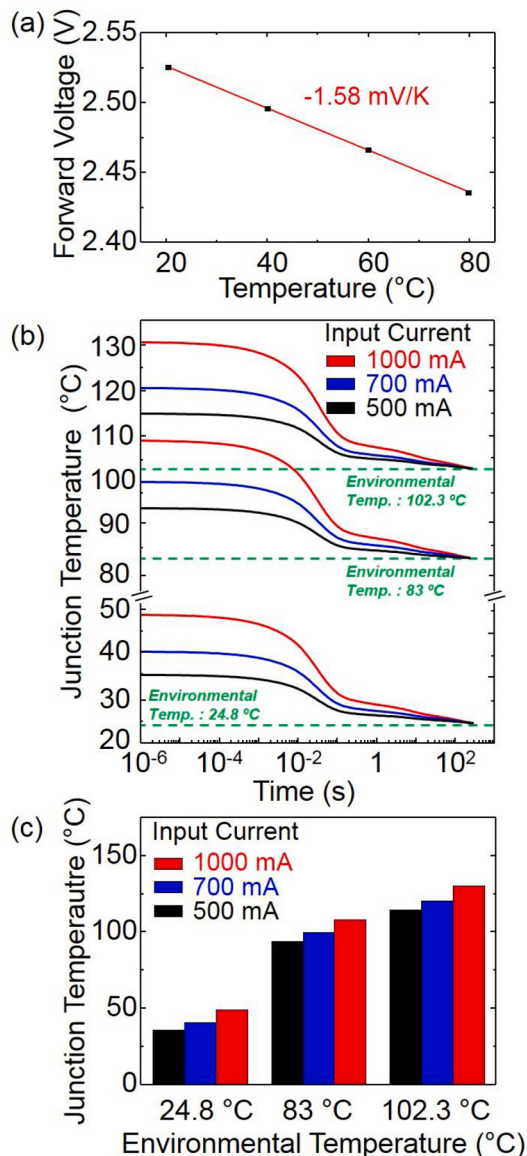


Fig. 2. Junction temperature measurement of LED operated at an elevated temperature. (a) Linear relationship between forward voltage and temperature measured by applying a small 0.1-mA forward current. (b) Recorded change in junction temperature immediately after turning off the LED (*i.e.*, cooling period) with respect to the input current (500, 700, and 1000 mA) and environmental temperature (24.8, 83, and 102.3 °C). The y-intercept indicates the measured junction temperature at each condition that eventually saturates down to the environmental temperature. (c) Characterized junction temperature of LED measured under various input currents and environmental temperatures.

3. Results and discussion

The LED junction temperature is measured using the T3Ster equipment at the environmental temperature range 24.8–102.3 °C. The thermal transient analysis of LED relies on the relationship between forward voltage and temperature; hence, the LED is placed in a thermostat, and a small forward current (0.1 mA) is applied. It should be noted that this input current is considerably smaller than the driving current of LED and does not contribute to the increase in junction temperature. As such, the temperature at the junction would be identical to that of the thermostat. The forward voltage is thereafter measured with respect to the thermostat temperature (*i.e.*, junction

temperature), as shown in Fig. 2(a). The junction temperature dependency on the forward voltage is measured to be -1.58 mV/K , which is subsequently employed to convert the measured forward voltage to junction temperature.

The LED junction temperature is measured during its cooling period. The LED is first turned on with forward currents of 500 mA (1.482–1.438 W), 700 mA (2.142–2.085 W), and 1000 mA (3.193–3.124 W) at environmental temperatures of 24.8, 83, and 102.3 °C to which the LED is exposed. Upon reaching the steady-state, the LED is turned off, and the input currents immediately reduce to 0.1 mA within $\sim 1 \mu\text{s}$. The forward voltage is concurrently measured with the 0.1-mA input current. Based on the relationship presented in Fig. 2(a), the change in the forward voltage is converted into junction temperature, as shown in Fig. 2(b). The y-intercepts (temperatures at 10^{-6} s) in Fig. 2(b) indicate the junction temperature measured under the applied currents and environmental temperatures. As summarized in Fig. 2(c), the increases in input current and temperature also increase the junction temperature as expected. The junction temperature is 35.63 °C at 500 mA forward current and 24.8 °C environmental temperature; however, it reaches up to 130.31 °C at 1000 mA and 102.3 °C. The temperature values at the junction are used as reference when compared with the phosphor and thermal pad temperatures measured under identical conditions.

The phosphor temperature is measured using an IR thermometer under the identical input current and environmental temperature used for junction temperature measurements. The IR camera is a useful tool for measuring the phosphor-converted white-light LED because there is no IR emission and interference from the LED [30]. The phosphor is composed of $\text{Y}_3\text{Al}_5\text{O}_{12}$ (YAG)-based material, which has a negligible transmittance over $\sim 6.4 \mu\text{m}$ wavelength [49,50]. It indicates that the phosphor is not IR transparent, and thus, its temperature can be measured, considering the spectral range (7.5–13 μm) of the IR camera used. In addition, the emissivity of phosphor should be considered, because the temperature value measured by the IR camera depends on material emissivity. Instead of directly measuring the emissivity of phosphor, which is temperature dependent and may require an additional complicated system, the IR camera is calibrated against the known phosphor temperature. For the calibration, the LED is placed inside the oven equipped with an IR transparent window, and the IR camera records the phosphor temperature. As the temperature inside the oven increases, it is measured by a thermocouple located near the LED. Under this condition, the phosphor temperature would be identical to that of the oven (*i.e.*, measured by the thermocouple) as no electrical power is applied to the LED. The linear correlation ($R^2 = 0.998$) between the actual phosphor temperatures and those measured by the IR camera is thus obtained, as shown in Fig. 3(a). This relationship is used for measuring the phosphor temperature of the LED operated at high environmental temperatures and various input currents using the IR camera. The presence of an encapsulating extraction lens would block the measurement of the phosphor temperature by the IR camera [51]. However, considering the LEDs that use monolithic phosphor resin [14], the IR camera could be still useful for the thermal characterization of the phosphor temperature of such an LED configuration.

Fig. 3(b) shows a transient temperature profile of the phosphor measured by the IR camera. The LED is turned on (at 60 s) and off (at 260 s) with input currents of 500, 700, and 1000 mA at environmental temperatures of 24.8, 83, and 102.3 °C. The phosphor temperature reaches a steady-state (*i.e.*, temperature fluctuations within ± 0.5 °C) within ~ 39 s at 1000 mA of input current and 102.3 °C of environmental temperature, immediately after the LED is turned on. The temperature differences between the on and off states gradually increase from 17.31 to 27.04 °C at an input current of 1000 mA as the environmental temperature increases. The measured maximum phosphor temperature is 129.34 °C at a 1000-mA input current and 102.3 °C environmental temperature. The insets in Fig. 3(b) show the captured

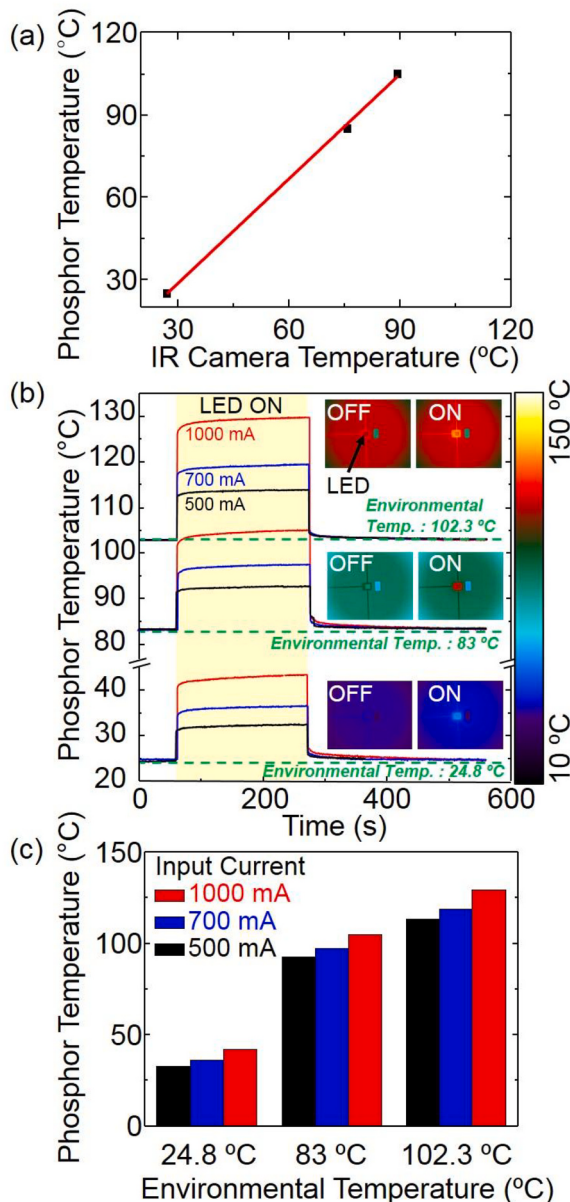


Fig. 3. Measurement of phosphor temperature of LED operated at elevated temperatures using an IR thermometer. (a) Linear relationship between the actual phosphor temperature and measured temperature by IR camera. This relationship is later used for the calibration of IR camera. (b) Real-time temperature change of phosphor temperature. The LED is turned on and off at 60 and 260 s, respectively, with different input currents (500, 700, and 1000 mA) at an environmental temperature in the range 24.8–102.3 °C. Insets show the captured IR images of the LED in off and on states (input current: 700 mA) at each environmental temperature. (c) Characterized phosphor temperature of LED measured at various input currents and environmental temperatures.

IR images at each environmental temperature before and after the LED is turned on at 700 mA; measurement results are summarized in Fig. 3(c). Similar to the junction temperature, the phosphor temperature also depends on the input current and environmental temperature. The maximum phosphor temperature is lower than that of the junction temperature under identical conditions possibly because of the additional heat transfer caused by natural air convection.

The temperature change at the thermal pad according to the on and off operations of the LED is investigated using a thermocouple. In general, the thermocouple is frequently used in the industry to estimate the junction temperature by measuring the temperature at a specific

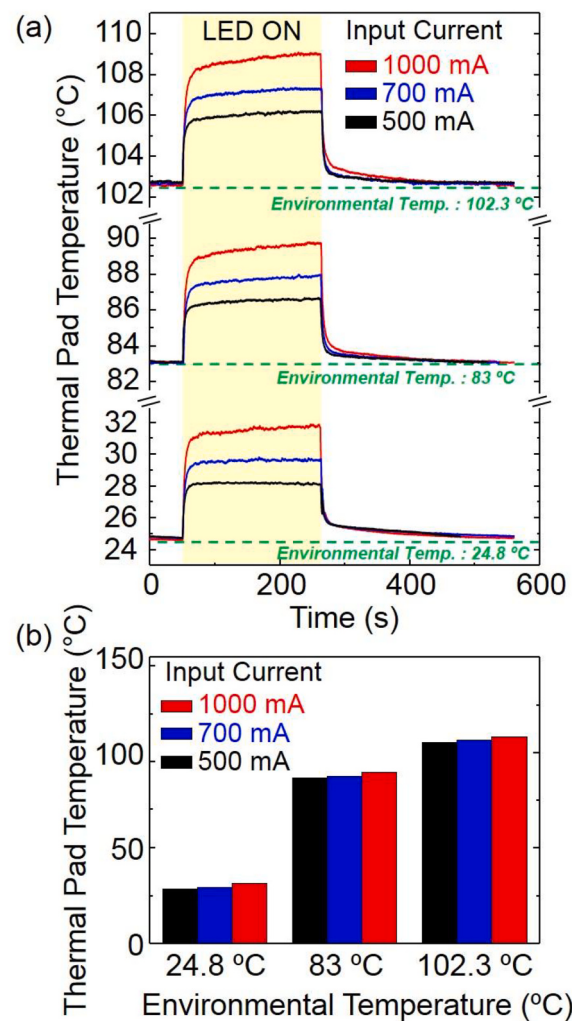


Fig. 4. Measurement of thermal pad temperature using thermocouple. (a) Real-time change in thermal pad temperature according to LED operation. (b) Characterized thermal pad temperature of LED measured at various input currents and environmental temperatures.

location where the thermal resistance at the junction is known. Identical to the junction and phosphor temperature measurements, the input current for the LED and environmental temperature are modulated, and the change in thermal pad temperature is recorded in real time. As shown in Fig. 4(a), the temperature at the thermal pad also varies according to the on and off operations of the LED. The time required to reach the steady-state at 1000 mA of input current and 102.3 °C of environmental temperature (~55 s) is relatively longer compared to that of the phosphor because of the higher thermal impedance from the junction to the thermal pad. Similar to the temperature changes at the junction and phosphor, the thermal pad temperature also gradually increases as the input current and environmental temperature increase (Fig. 4(b)). The thermal pad temperature, however, is lower than those of the junction and phosphor under identical conditions, e.g., the maximum temperature is 108.41 °C at a 1000-mA input current and 102.3 °C environmental temperature.

Based on the experimental results on temperature measurements, the junction–phosphor and junction–thermal pad correlations are found. As shown in Fig. 5(a), the junction temperature exhibits a single and highly linear correlation ($R^2 = 0.997$) against the phosphor temperature regardless of input currents at an environmental temperature reaching up to 107.2 °C. In order to find this correlation, the junction and phosphor temperatures were measured by identical procedures as

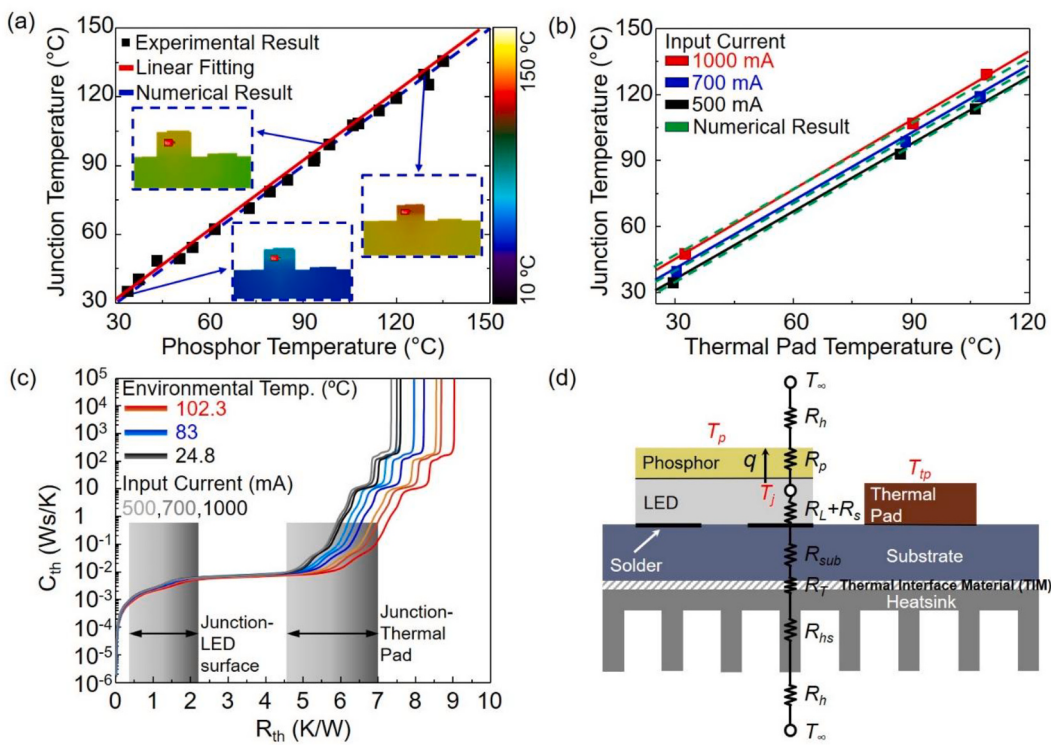


Fig. 5. Correlation between junction temperature and phosphor and thermal pad temperatures of LED operated at an elevated temperature. (a) Single and linear correlation ($R^2 = 0.997$) between the junction and phosphor temperatures measured up to an environmental temperature of $107.2\text{ }^\circ\text{C}$. Based on this correlation, the junction temperature can be precisely determined by measuring the phosphor temperature. The black filled squares and red solid line represent experimental data and linear fitting, respectively. The blue dotted line denotes the numerical results obtained using a commercial solver (ANSYS 19.2). The insets show the exemplary numerical results for the LED temperature contours. (b) Input current-dependent linear correlations ($R^2 = 0.999$ for all tested input currents (*i.e.*, 500, 700, and 1000 mA)) between the junction and thermal pad temperatures. Both input current and operating temperature must be considered when the junction temperature is predicted based on the thermal pad temperature. The filled objects and solid lines represent experimental data and linear fitting, respectively. (c) Cumulative structure function of LED operated at various input currents and environmental temperatures. The thermal resistance of each component from the LED junction can be found. The shaded regions indicate the experimentally measured thermal resistance from the junction to the LED surface (phosphor) and thermal pad. (d) One-dimensional heat transfer through multilayers and electrical analogy for LED junction temperature calculation. (For interpretation of the references to color in this figure legend, the reader is referred to the web version of this article.)

previously presented against various input currents and environmental temperatures (Fig. S1 and S2, Supporting Information). The single linear correlation indicates that the LED junction temperature exposed to a high environmental temperature can be accurately predicted by simply measuring the temperature on the phosphor surface without the use of a complicated equipment. In our experimental condition, the phosphor temperature is averagely $\sim 97.37\%$ lower than the junction temperature. The insets in Fig. 5(a) show the temperature contours of the LED package that are derived from a steady-state numerical analysis with the measured junction temperature as a primary heat source under natural convection. The temperature-dependent thermal conductivities of GaN LED and Al substrate/heatsink were used for numerical analysis [52–55], while the thermal conductivities of phosphor (Nd:YAG), solder (SAC305), thermal pad (Cu), dielectric (HPL-03015), and thermal interface material (TIM) were set as 12, 58, 398, 7.5, and 1.1 W/(m K), respectively. The experimental and numerical results are consistent (differences are within $\sim 2.9\%$).

Different from the correlation between the junction and phosphor temperatures, the thermal pad temperature shows input current-dependent multiple linear correlations ($R^2 = 0.999$ for all tested input currents: 500, 700, and 1000 mA) with the junction temperature (Fig. 5(b)). In typical industrial fields, these multiple correlations are frequently ignored and treated as a single correlation. If the LED is operated at a constant environmental temperature, a single correlation between them can be found and used. The experimental results herein, however, imply that the prediction of junction temperature from the thermal pad temperature should consider the input current when the

LED is operated at varying environmental temperatures. The numerical analysis also supports the experimental results. For different LED designs and products, these temperature correlations between the junction and the other parts of LED should also be found by experiments. Once the temperature correlation is found, it can be applicable for all products that adopt the identical LED design.

To verify the experimental results, the thermal resistance of the LED package is measured and characterized using T3Ster. The heat generated at the junction is dissipated via conductive heat transfer to the bottom of the LED package, and the difference in thermal properties among the LED component results in distinguishable thermal impedance [31]. The cumulative thermal capacitance is thus found against the thermal resistance from the junction to the bottom of the LED package (*i.e.*, heat sink) according to the input currents and environmental temperatures (Fig. 5(c)). The increases in input current and environmental temperature result in higher power dissipation, thereby leading a higher self-heating. These structure functions of the LED package allow the identification of the thermal resistance of LED die, solder, substrate, TIM, and heatsink (Table S1, Supporting Information). For example, the thermal resistances between the junction–outer surface of LED die and junction–thermal pad (*i.e.*, junction–top of substrate) are estimated as $\sim 0.34\text{--}0.47$ and $\sim 5.1\text{--}6.3$ K/W, respectively. Additionally, the thermal resistances are calculated based on the experimental results of temperature measurements at the junction, phosphor, and thermal pad at a given input power. The shaded regions in Fig. 5(c) indicate the calculated thermal resistance from the junction to the LED surface (phosphor) ($\sim 0.31\text{--}2.13$ K/W) and thermal pad

(~4.64–7.01 K/W), which correspond to the structure function of the LED measured by T3Ster.

Fig. 5(d) depicts the one-dimensional heat transfer model using an equivalent network for thermal resistance analysis. Its mathematical representation can be given by the following relationship:

$$q = \frac{T_j - T_\infty}{R_p + R_h} + \frac{T_j - T_\infty}{R_L + R_s + R_{sub} + R_T + R_{hs} + R_h}$$

where q is the heat flux [W]; T is the temperature [K]; R is the thermal resistance [K/W]; subscripts j , p , L , s , sub , T , hs , and h denote the junction, phosphor, LED die, solder, substrate, TIM, heatsink, and convective heat transfer, respectively. In this model, we assume the thermal resistance between the top of substrate and the thermal pad is negligible, which is similar to the one-dimensional thermal behavior obtained from the cumulative structure function. On the other hand, as the structure function only allows the measurement of thermal resistance from the junction to the bottom, the thermal resistance of phosphor is not directly accessible or often treated to be identical to that of the LED surface in the transient thermal test. Given the above equation and the thermal resistance values, the thermal conductivity of the phosphor can be found. The thermal conductivity of phosphor decreases from 12.77 to 9.99 W/(m K) when the phosphor temperature increases from 32.75 to 129.34 °C (Table S2, Supporting Information). These analyses imply that the thermal resistance inside the LED can be significantly changed according to the amount of self-heating and the temperature-dependent thermal conductivity of the component. Such dependency should therefore be considered for the estimation of junction temperature based on the temperature measurement of other components, especially when the LED is operated at high temperatures.

4. Conclusions

The temperature profiles of the LED operated at high-temperature environments for precise junction temperature measurement are characterized. The junction, phosphor, and thermal pad temperatures are measured using different equipment, such as transient thermal tester, IR thermometer, and thermocouple at an environmental temperature and input current of up to 107.2 °C and 1000 mA, respectively. A series of experiments demonstrates a single highly linear correlation between the junction and phosphor temperatures, enabling accurate estimation of the junction temperature by simply measuring the temperature on the phosphor surface, which is not encapsulated by a lens, without employing complicated equipment and procedure. Moreover, the input current-dependent linear correlation between the junction and thermal pad temperatures are found. The junction temperature is usually predicted from the thermal pad temperature, which is measured by the thermocouple, based on known input power and thermal resistance by assuming a single correlation between the two. The findings herein, however, indicate that the input current should be considered for estimating the junction temperature from the thermal pad temperature when the LED is operated at varying environmental temperatures. The above experimental results are supported by the thermal resistance analysis of the LED package. Considering the increasing demands for high-power LED in automotive lighting, the precise measurement of the junction temperature could be a starting point for the successful thermal management of LEDs. This can be useful in preventing failure and maintaining the performance of LED-based products.

Declaration of Competing Interest

The authors declare that they have no known competing financial interests or personal relationships that could have appeared to influence the work reported in this paper.

Acknowledgements

This research was supported by the Basic Science Research Program through the National Research Foundation of Korea (NRF), funded by the Ministry of Education (2019R1F1A1058411) and by the Ministry of Science, ICT and Future Planning (2019R1C1C1007840). This research was also supported by Korea Institute for Advancement of Technology (KIAT) grant funded by the Korea Government (MOTIE) (P0002092, The Competency Development Program for Industry Specialist).

Appendix A. Supplementary data

Supplementary data to this article can be found online at <https://doi.org/10.1016/j.mee.2020.111451>.

References

- [1] E.F. Schubert, J.K. Kim, Solid-state light sources getting smart, *Science* 308 (5726) (2005) 1274–1278.
- [2] X. Luo, R. Hu, S. Liu, K. Wang, Heat and fluid flow in high-power LED packaging and applications, *Prog. Energy Combust. Sci.* 56 (2016) 1–32.
- [3] X. Long, J. He, J. Zhou, L. Fang, X. Zhou, F. Ren, T. Xu, A review on light-emitting diode based automotive headlamps, *Renew. Sust. Energ. Rev.* 41 (2015) 29–41.
- [4] M. Hamidnia, Y. Luo, X. Wang, Application of micro/nano technology for thermal management of high power LED packaging—a review, *Appl. Therm. Eng.* 145 (2018) 637–651.
- [5] M.H. Chang, D. Das, P.V. Varde, M. Pecht, Light emitting diodes reliability review, *Microelectron. Reliab.* 52 (5) (2012) 762–782.
- [6] J. Park, C.C. Lee, An electrical model with junction temperature for light-emitting diodes and the impact on conversion efficiency, *IEEE Electron Device Lett.* 26 (5) (2005) 308–310.
- [7] Y. Lai, N. Cordero, F. Barthel, F. Tebbe, J. Kuhn, R. Apfelbeck, D. Würtenberger, Liquid cooling of bright LEDs for automotive applications, *Appl. Therm. Eng.* 29 (5–6) (2009) 1239–1244.
- [8] X. Lin, S. Mo, L. Jia, Z. Yang, Y. Chen, Z. Cheng, Experimental study and Taguchi analysis on LED cooling by thermoelectric cooler integrated with microchannel heat sink, *Appl. Energy* 242 (2019) 232–238.
- [9] J. Jiang, J.E. Lee, K.S. Kim, K. Suganuma, Oxidation behavior of Sn–Zn solders under high-temperature and high-humidity conditions, *J. Alloys Compd.* 462 (1–2) (2008) 244–251.
- [10] J. Hu, L. Yang, M.W. Shin, Mechanism and thermal effect of delamination in light-emitting diode packages, *Microelectron. J.* 38 (2) (2007) 157–163.
- [11] G. Elger, S.V. Kandaswamy, E. Liu, A. Hanss, M. Schmid, R. Derix, F. Conti, Analysis of solder joint reliability of high power LEDs by transient thermal testing and transient finite element simulations, *Microelectron. J.* 46 (12, 2015) 1230–1238.
- [12] G. Elger, D. Müller, A. Hanß, M. Schmid, E. Liu, U. Karbowski, R. Derix, Transient thermal analysis for accelerated reliability testing of LEDs, *Microelectron. Reliab.* 64 (2016) 605–609.
- [13] P.F. Smet, A.B. Parmentier, D. Poelman, Selecting conversion phosphors for white light-emitting diodes, *J. Electrochem. Soc.* 158 (6) (2011) R37–R54.
- [14] Q. Chen, Y. Ma, X. Yu, R. Hu, X. Luo, Phosphor temperature overestimation in high-power light-emitting diode by thermocouple, *IEEE Trans. Electron Devices* 64 (2) (2016) 463–466.
- [15] X. Luo, X. Fu, F. Chen, H. Zheng, Phosphor self-heating in phosphor converted light emitting diode packaging, *Int. J. Heat Mass Transf.* 58 (1–2) (2013) 276–281.
- [16] X. Luo, R. Hu, Calculation of the phosphor heat generation in phosphor-converted light-emitting diodes, *Int. J. Heat Mass Transf.* 75 (2014) 213–217.
- [17] T.Y. Chung, S.C. Chiou, Y.Y. Chang, C.C. Sun, T.H. Yang, S.Y. Chen, Study of temperature distribution within pc-WLEDs using the remote-dome phosphor package, *IEEE Photon. J.* 7 (2) (2015) 8200111.
- [18] D. Jang, S.H. Yu, K.S. Lee, Multidisciplinary optimization of a pin-fin radial heat sink for LED lighting applications, *Int. J. Heat Mass Transf.* 55 (4) (2012) 515–521.
- [19] Q. Shen, D. Sun, Y. Xu, T. Jin, X. Zhao, Orientation effects on natural convection heat dissipation of rectangular fin heat sinks mounted on LEDs, *Int. J. Heat Mass Transf.* 75 (2014) 462–469.
- [20] E. Jung, Y. Lee, Development of a heat dissipating LED headlamp with silicone lens to replace halogen bulbs in used cars, *Appl. Therm. Eng.* 86 (2015) 143–150.
- [21] X.J. Zhao, Y.X. Cai, J. Wang, X.H. Li, C. Zhang, Thermal model design and analysis of the high-power LED automotive headlight cooling device, *Appl. Therm. Eng.* 75 (2015) 248–258.
- [22] C.H. Huang, G.J. Wang, A design problem to estimate the optimal fin shape of LED lighting heat sinks, *Int. J. Heat Mass Transf.* 106 (2017) 1205–1217.
- [23] B. Yan, N.T. Tran, J.P. You, F.G. Shi, Can junction temperature alone characterize thermal performance of white LED emitters? *IEEE Photon. Technol. Lett.* 23 (9) (2011) 555–557.
- [24] K. Chen, B. Lin, H. Chen, M. Shih, C. Wang, H. Kuo, H. Tsai, M. Kuo, S. Chien, P. Lee, Effect of the thermal characteristics of phosphor for the conformal and remote structures in white light-emitting diodes, *IEEE Photonics J.* 5 (5) (2013) 8200508.
- [25] X. Fu, X. Luo, Can thermocouple measure surface temperature of light emitting

- diode module accurately? *Int. J. Heat Mass Transf.* 65 (2013) 199–202.
- [26] S. Todoroki, M. Sawai, K. Aiki, Temperature distribution along the striped active region in high-power GaAlAs visible lasers, *J. Appl. Phys.* 58 (3) (1985) 1124–1128.
- [27] Y. Gu, N. Narendran, A noncontact method for determining junction temperature of phosphor-converted white LEDs, *Proc. SPIE* 5187 (2004) 107–114.
- [28] Y. Ma, R. Hu, X. Yu, W. Shu, X. Luo, A modified bidirectional thermal resistance model for junction and phosphor temperature estimation in phosphor-converted light-emitting diodes, *Int. J. Heat Mass Transf.* 106 (2017) 1–6.
- [29] E. Tamdogan, G. Pavlidis, S. Graham, M. Arik, A comparative study on the junction temperature measurements of LEDs with raman spectroscopy, microinfrared (IR) imaging, and forward voltage methods, *IEEE Trans. Compon. Packag. Manuf. Technol.* (99) (2018) 1–9.
- [30] D. Lee, H. Choi, S. Jeong, C.H. Jeon, D. Lee, J. Lim, C. Byon, J. Choi, A study on the measurement and prediction of LED junction temperature, *Int. J. Heat Mass Transf.* 127 (2018) 1243–1252.
- [31] V. Székely, A new evaluation method of thermal transient measurement results, *Microelectron. J.* 28 (3) (1997) 277–292.
- [32] Y. Xi, E. Schubert, Junction-temperature measurement in GaN ultraviolet light-emitting diodes using diode forward voltage method, *Appl. Phys. Lett.* 85 (12, 2004) 2163–2165.
- [33] Y. Xi, J.Q. Xi, T. Gessmann, J. Shah, J. Kim, E. Schubert, A. Fischer, M. Crawford, K. Bogart, A. Allerman, Junction and carrier temperature measurements in deep-ultraviolet light-emitting diodes using three different methods, *Appl. Phys. Lett.* 86 (3) (2005) 031907.
- [34] A. Keppens, W. Ryckaert, G. Deconinck, P. Hanselaer, High power light-emitting diode junction temperature determination from current-voltage characteristics, *J. Appl. Phys.* 104 (9) (2008) 093104.
- [35] Y.J. Lee, C.J. Lee, C.H. Chen, Determination of junction temperature in InGaN and AlGaN/P light-emitting diodes, *IEEE J. Quantum Electron.* 46 (10, 2010) 1450–1455.
- [36] Q. Chen, X. Luo, S. Zhou, S. Liu, Dynamic junction temperature measurement for high power light emitting diodes, *Rev. Sci. Instrum.* 82 (8) (2011) 084904.
- [37] X. Tao, H. Chen, S.N. Li, S.R. Hui, A new noncontact method for the prediction of both internal thermal resistance and junction temperature of white light-emitting diodes, *IEEE Trans. Power Electron.* 27 (4) (2012) 2184–2192.
- [38] H. Choi, W. Choi, J. Lim, J. Choi, Integrated microsensor for precise, real-time measurement of junction temperature of surface-mounted light-emitting diode, *Sens. Actuators A* 298 (2019) 111578.
- [39] S. Chhajed, J. Cho, E.F. Schubert, J.K. Kim, D.D. Koleske, M.H. Crawford, Temperature-dependent light-output characteristics of GaInN light-emitting diodes with different dislocation densities, *Phys. Status Solidi A* 208 (4) (2011) 947–950.
- [40] C.M. Tan, P. Singh, Time evolution degradation physics in high power white LEDs under high temperature-humidity conditions, *IEEE Trans. Device Mater. Reliab.* 14 (2) (2014) 742–750.
- [41] J. Huang, D.S. Golubović, S. Koh, D. Yang, X. Li, X. Fan, G. Zhang, Lumen degradation modeling of white-light LEDs in step stress accelerated degradation test, *Reliab. Eng. Syst. Saf.* 154 (2016) 152–159.
- [42] M. Cai, D. Yang, J. Zheng, Y. Mo, J. Huang, J. Xu, W. Chen, G. Zhang, X. Chen, Thermal degradation kinetics of LED lamps in step-up-stress and step-down-stress accelerated degradation testing, *Appl. Therm. Eng.* 107 (2016) 918–926.
- [43] M. Meneghini, L.R. Trevisanello, U. Zehnder, T. Zahner, U. Strauss, G. Meneghesso, E. Zanoni, High-temperature degradation of GaN LEDs related to passivation, *IEEE Trans. Electron Devices* 53 (12, 2006) 2981–2987.
- [44] M. Meneghini, A. Tazzoli, G. Mura, G. Meneghesso, E. Zanoni, A review on the physical mechanisms that limit the reliability of GaN-based LEDs, *IEEE Trans. Electron Devices* 57 (1) (2010) 108–118.
- [45] M. Dal Lago, M. Meneghini, N. Trivellin, G. Meneghesso, E. Zanoni, Degradation mechanisms of high-power white LEDs activated by current and temperature, *Microelectron. Reliab.* 51 (9–11) (2011) 1742–1746.
- [46] M. Meneghini, M. Dal Lago, N. Trivellin, G. Meneghesso, E. Zanoni, Degradation mechanisms of high-power LEDs for lighting applications: an overview, *IEEE Trans. Ind. Appl.* 50 (1) (2014) 78–85.
- [47] J. Huang, D.S. Golubović, S. Koh, D. Yang, X. Li, X. Fan, G. Zhang, Degradation mechanisms of mid-power white-light LEDs under high-temperature–humidity conditions, *IEEE Trans. Device Mater. Reliab.* 15 (2) (2015) 220–228.
- [48] See <https://www.mentor.com/products/mechanical/micred/t3ster/> for T3Ster.
- [49] J. Li, Q. Chen, G. Feng, W. Wu, D. Xiao, J. Zhu, Optical properties of the polycrystalline transparent Nd:YAG ceramics prepared by two-step sintering, *Ceram. Int.* 38S (2012) S649–S652.
- [50] L.-L. Wang, L. Mei, G. He, G.-H. Liu, J.-T. Li, L.-H. Xu, Z.-J. Jiang, Preparation of infrared transparent YAG-based glass-ceramics with nano-sized crystallites, *J. Eur. Ceram. Soc.* 32 (2012) 3091–3096.
- [51] T.-H. Yang, H.-Y. Huang, C.-C. Sun, B. Glorieux, X.-H. Lee, Y.-W. Yu, T.-Y. Chung, Noncontact and instant detection of phosphor temperature in phosphor-converted white LEDs, *Sci. Rep.* 8 (2018) 296.
- [52] K. Ahmeda, B. Ubochi, B. Benbatli, S.J. Duffy, A. Soltani, W.D. Zhang, K. Kalna, Role of self-heating and polarization in AlGaN/GaN-based heterostructures, *IEEE Access* 5 (2017) 20946–20952.
- [53] C. Mion, J.F. Muth, E.A. Preble, D. Hanser, Accurate dependence of gallium nitride thermal conductivity on dislocation density, *Appl. Phys. Lett.* 89 (2006) 092123.
- [54] H. Shibata, Y. Waseda, H. Ohta, K. Kiyomi, K. Shimoyama, K. Fujito, H. Nagaoaka, Y. Kagamitani, R. Simura, T. Fukuda, High thermal conductivity of gallium nitride (GaN) crystals grown by HVPE process, *Mater. Trans.* 48 (10) (2007) 2782–2786.
- [55] R.W. Powell, C.Y. Ho, P.E. Liley, Thermal Conductivity of Selected Materials, U.S. Dept. of Commerce, National Bureau of Standards, Washington, 1966.

Hyunjin Choi received the M.S. degree in the School of Mechanical Engineering from Yeungnam University, Republic of Korea. His research interest is thermal characterization of optoelectronic devices. He is currently working for SL corporation.

Leilei Wang is a Ph.D. student in the School of Mechanical Engineering at Yeungnam University, Republic of Korea. Her research interest is nanomaterial-based soft sensors.

Seok-Won Kang received the M.S. degree in Mechanical Aerospace & Systems Engineering from KAIST, Daejeon, Republic of Korea, in 2007, and the Ph.D. degree in Mechanical Engineering from Texas A&M University, College Station, TX, USA, in 2012. From 2012 to 2018, he was a Senior Researcher in the Metropolitan Transportation Research Center at Korea Railroad Research Institute, Uiwang, Republic of Korea. Currently, he is an Assistant Professor in the Department of Automotive Engineering at Yeungnam University, Gyeongsan, Republic of Korea. His research interests include green and intelligent vehicle systems, micro/nano-scale thermo-fluidics, and numerical methods in engineering.

Jiseok Lim received the M.S. degree and Ph.D. degrees in mechanical engineering from Yonsei University, Seoul, Republic of Korea, in 2006 and 2011, respectively. He has worked for Max Planck Institute, Goettingen, Germany, where he was involved in several interdisciplinary research projects at the interfaces between physics, biochemistry and mechanical engineering. Since 2015, he has been an Assistant Professor with the School of Mechanical Engineering, Yeungnam University, Gyeongbuk, Republic of Korea. His research interests include optical system, enzyme biochemistry, and precision manufacturing.

Jungwook Choi received the BS and PhD degrees in Mechanical Engineering from Yonsei University, Korea in 2006 and 2013, respectively. He worked as a postdoctoral research associate at Purdue University from 2014 to 2016. He then joined the School of Mechanical Engineering at Yeungnam University as an assistant professor. His current research focuses on modeling, design, and fabrication of nanomaterial-integrated micro/nanosystems.